Hybrid LC Filter Electrical Design Considerations

Valentin Dzhankhotov, Juha Pyrhönen, *Member, IEEE,* Pertti Silventoinen, and Mikko Kuisma

***Abstract*— This paper continues design considerations of the novel type of passive filter called hybrid LC filter (HLCF). The filter is aimed for significant reduction of high frequency differential mode (DM) and common mode (CM) currents in speed controlled AC drives. A model of the HLCF is presented. Based on the model, a transfer function of the HLCF is found. The hybrid LC filter behaviour is analyzed in frequency domain. Based on the provided analysis, possible implementations of the HLCF technology are analysed. A method for the HLCF frequency domain behaviour estimation with asymptotes is proposed. Comparison of the measured, simulated and calculated results in frequency domain is presented.**

***Index Terms*—high-power drives, filters, common mode, differential mode, overvoltage.**

I. Introduction

Power electronic converter drives use, for the sake of high efficiency, pulse-width modulation (PWM) that results in sequences of high-voltage high-frequency steep-edged pulses. Such a power signal contains a set of high harmonics which are not required for control purposes but, instead, create harmful effects. Harmonics cause reflections in the cable between the motor and the inverter leading to faster winding insulation ageing [1]–[8]. Bearing failures and problems with electromagnetic compatibility may also result [9]–[15].

Electrical d*u*/d*t* filters provide an effective solution to problems caused by pulse-width modulation, thereby increasing the performance and service life of the electrical machines. It is shown, for example, in [1] –[3], [6], [16] and [17] that RLC filters effectively decrease differential- and common-mode noises leading to motor winding insulation breakdowns and bearings damages.

Foil chokes and film capacitors are among the most widely used components in high-power applications. In actual applications they can be placed in different parts of the cabinet. This fact complicates the arrangement of the cabinet and decreases the reliability of the system. In addition, the inductances of connection wires may prevent filtration at high frequencies.

In [1], [2], [18] and [19] a new hybrid LC filter was introduced. This filter uses the natural capacitance between the turns of the foil choke based on integration of an auxiliary layer into it (Fig. 1).

The main idea of the hybrid LC filter results from the fact that both the foil choke and the film capacitors have the same roll structure. Moreover, the capacitance between the turns ("intra capacitance" often referred to an end-to-end capacitance) of the foil inductors is the reason for the deterioration of choke properties at high frequencies [20]. It is shown in [1] and [2] that the proposed filter has a natural cancellation of the intra capacitance. A hybrid LC filter may contain two or more foil layers isolated from each other and coiled on a core. The core material can be ferromagnetic material such as iron lamination, air or a suitable combination of them. In this paper an air cored hybrid filter is observed. Therefore, no eddy currents are present in the core. In iron cores the eddy currents at high frequencies should significantly affect the attenuation behavior of the filter.

Foils carrying the useful power signal, called the main foils, are placed between the inverter and the motor cable. Other ones, called auxiliary foils, may be connected in star to create differential- and common-mode noises paths. The star point is then coupled to the DC link midpoint to guarantee a

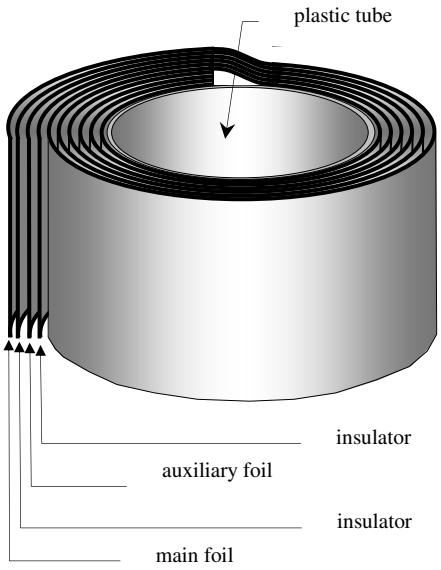

Fig. 1. Single-phase column of the proposed hybrid LC filter.

Manuscript received September 9, 2010. Accepted for publication May 2, 2011.

V. Dzhankhotov is now with The Switch Drive Systems Oy, Lappeenranta, CO 53850, Finland (e-mail: valentin.dzhankhotov@theswitch.com). He is also with Lappeenranta University of Technology, Lappeenranta, CO 53850 Finland.

J. Pyrhönen, P. Silventoinen, M. Kuisma and T. Minav are now with the Department of Electrical Engineering, Lappeenranta University of Technology, Lappeenranta, CO 53850 Finland (e-mail: juha.pyrhonen@lut.fi).

travelling path, especially for the common-mode currents. There is a remarkable capacitance between the main foil and the auxiliary foil.

The proposed LC filter can be a competitive solution for modern power drives and offers advantages over the traditional chokes and filters. It has good DM and CM noise attenuation properties. As a single unit, the HLCF provides equal or better reliability compared with the filters based on separate components. Because of the natural capacitance, no extra connections producing the high-frequency operation deterioration are required. The filter works for both differential and common modes, maintains its inductance at high frequencies, and has good cooling properties because of the air core letting cooling fluid flow easily. If needed, the low-frequency inductance can be increased by ferromagnetic core parts. The auxiliary foil also minimizes the intra capacitance of the main foil [2].

The reliability of the HLCF can be assumed approximately equal to or lower than the reliability of a foil choke. The voltage stresses are higher in the HLFC than in a foil choke because the auxiliary foil has a low potential, and therefore, the electric field strength is high between the main and aux foils. In conventional foil chokes, the insulation is significantly less stressed because the potential differences between the turns are rather small.

Usually, the current flowing through the capacitance of a du/dt filter is considerably smaller than the current flowing through the choke. Moreover, the losses depend on the current squared. Thus, for both a conventional LC filter and the HLCF capacitive chain, losses are negligibly low. Therefore, both types of filters can be described by an equal amount of losses, which are quite close to the losses in a traditional air-cored choke.

The disadvantage of the HLCF is the slightly more complicated manufacturing technology when using the present-day fabrication facilities. However, rolling four layers (main foil, insulation, auxiliary foil, insulation) simultaneously instead of two should not be too difficult. If manufacturing technology should be further developed, insulation bands integrated with the aux coil material might be possible. Then, the coil manufacturing should not differ from present day foil coil manufacturing except auxiliary foil connections.

On the other hand, the capacitors in three-phase passive power filters with separate components usually cost up to 50 % of the inductor price. The hybrid LC filter auxiliary foil can be made of a very thin material, because the common-mode currents are small. The amount of insulation, however, is larger than in traditional foil filters because thicker insulation layers must be used due to the high electric field strength. The price of the HLCF is expected to be about 0–25 % higher than the price of the chokes in filters based on separate components.

The main restrictions on the scalability of voltage and current ratings are similar to those for foil wound chokes. When increasing the voltage rating, special attention should be paid to the insulation properties. When increasing the current rating, the current density in the main foil as well as the insulation thermal properties must be carefully considered.

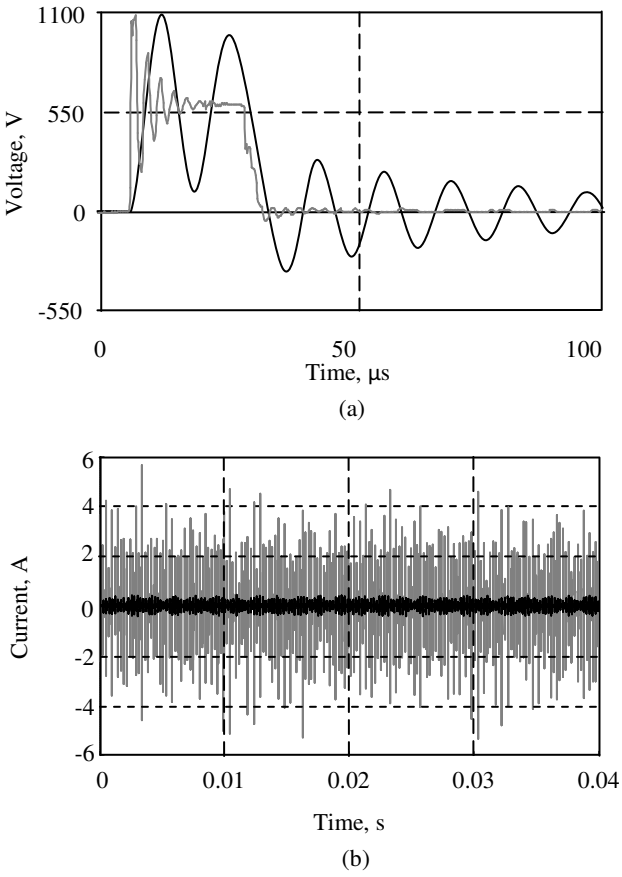

Fig 2. Phase to phase voltage (a) and common-mode (b) current in real drive: ━ – with the hybrid LC filter, ━ – without hybrid LC filter.

Fig. 2 shows measured phase to phase voltage and the common-mode currents in a drive when tested with the hybrid LC filter or without it. A 22 kW, 400 V, three-phase induction motor is driven by an ABB inverter with a PWM switching frequency of 2.4 kHz. The motor is connected to the inverter by a 90 m symmetric three-phase cable. The main parameters of the cable are: the DC resistance at 20 ºC is 0.524 Ω/km, the phase AC resistance at 50 Hz is 0.63 Ω/km, the phase inductance is 0.26 mH/km, and the operating capacitance is 0.55 μF/km. The inductance of the HLCF main and auxiliary foils is $L_m = L_a = 30$ μH and the capacitance between the main and auxiliary layers is C_b = 140 nF. The cabinet was manufactured of aluminium, which effectively guaranteed EMC. The topology proposed in [9] was implemented and a wire connecting the filter star point to the DC link midpoint was used. The measurements were made with a Yokogawa PZ4000 power analyzer, which provides a measurement frequency bandwidth up to 2 MHz. Differential voltage probes Testec TT-SI9002 with a frequency bandwidth up to 25 MHz were used for voltage measurements. A custom-made Rogowski coil with an estimated frequency bandwidth up to 5 MHz was used for the current measurements.

The hybrid LC-filter increases the pulse rise time by a factor of 25 (from 0.12 μs to 3 μs) and decreases the du/dt rate by a factor of 20 (from 5200 V/μs to 260 V/μs) compared with the case without filtering. Oscillations are explained by the

fact that no damping elements were used, which underlines the LC nature of the filter under consideration. As well, hybrid LC filter essentially decreases the common-mode noise with attenuation about 22 dB (from 6A to 0.5A).

This paper deals with the hybrid LC filter electrical design and modelling. Based on the model proposed in [1], the transfer function of the hybrid LC filter is found. This function is used during the frequency behavior analysis to find the resonance frequencies of the HLCF. Finally, comparison of the measured, simulated and calculated data is provided. The results show the degree of the realism of the proposed model and the transfer function as well as effectiveness of the HLCF behavior prediction by calculations.

II. Hybrid LC Filter Model

The lumped model of the hybrid LC filter is proposed in [1] and is proven with three prototypes. The model seems to be realistic for both time and frequency (up to at least 100 MHz) domains. This model is presented in Fig. 3.

The main foil with inductance L_m is coupled with the auxiliary foil with inductance L_a through the capacitance C_b and mutual inductance M.

The stray self-capacitances ('intra capacitances') of the main (C_{i1}) and the auxiliary (C_{i2}) foils are placed in parallel with the inductances of the main and auxiliary foils. It is shown in [2] that the intra capacitance of the main foil is effectively cancelled by the auxiliary foil. The ways of inductances L_m and L_a, capacitance C_b and intra capacitance without auxiliary foil calculation are shown in [1] and [2]. Studies in [1] proved that earthing of the auxiliary foil reduces the intra capacitance C_{i1} approximately to $1/15^{th}$, whereas the intra capacitance C_{i2} may be assumed unchanged, and the magnetic coupling factor between the main and the auxiliary foils even with nonprofessional winding rolling obtains values in the range $c = 0.9–0.98$.

III. Transfer Function

To find a transfer function of the system with the mutual inductance presented in Fig. 3 manually is not simple. Special programs for the symbolic calculations can be used. In our case we used the Maxima program currently developed by volunteer contributors under the General Public License.

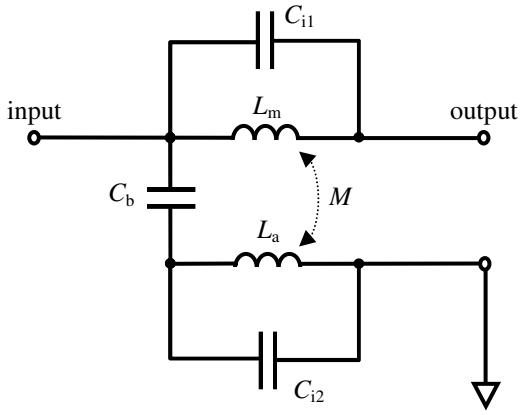

Fig 3. Lumped model of the hybrid LC filter.

The method of the transfer function definition for the circuits with mutual inductance is presented in [21]. First we have to redraw Fig. 3 to Fig. 4 taking into account the voltage source U_{in} with its internal resistance R_{in}, as well as a resistance R_{out} representing a load.

Let us select four independent circuits inside the main circuit and choose current directions in them as indicated in Fig. 4.

Now we can write the quadratic matrix of the impedances **A** (1). The number of row in this matrix corresponds to the number of the independent circuit inside the main electrical circuit of the hybrid LC filter, whereas the number of column corresponds to the current in the independent circuit with this number.

The matrix of voltages **B** (2) is written so that it indicates whether a voltage source exists in the independent circuit (by one) or not (by zero). The number of rows is again indicating the number of the independent circuit.

The next step is to find the inverse of matrix **A** and multiply this inverse matrix by matrix **B**. The result of these operations contains the transfer functions of the currents in

$$\mathbf{A} = \begin{bmatrix} R_{in} + \frac{1}{C_b s} + \frac{1}{C_{i2} s} & -\frac{1}{C_b s} & 0 & -\frac{1}{C_{i2} s} \\ -\frac{1}{C_b s} & \frac{1}{C_b s} + (L_m + L_a - 2M)s + R_{out} & L_m s + Ms & -L_a s + Ms \\ 0 & -L_m s + Ms & L_m s + \frac{1}{C_{i1} s} & -Ms \\ -\frac{1}{C_{i2} s} & -L_a s + Ms & -Ms & L_a s + -\frac{1}{C_{i2} s} \end{bmatrix} \quad (1)$$

$$\mathbf{B} = \begin{bmatrix} 1 \\ 0 \\ 0 \\ 0 \end{bmatrix} \quad (2)$$

each independent circuit, including current I_2 which creates the output voltage U_{out} across the resistor R_{out}. Since the whole result is bulky, it is skipped here. Instead, the transfer function $W_{out}(s)=\frac{U_{out}(s)}{U_{in}(s)}=\frac{I_2(s)R_{out}}{U_{in}(s)}$ is presented by (3).

IV. Transfer Function Analysis

Let us consider the HLCF behaviour across the frequency range from 0.1 Hz to 0.1 GHz. Now, let us think that $R_{in} = 0$, $R_{out} = \infty$ and $L_m = L_a = L$.

An asymptotic Bode plot is presented in Fig. 5. The frequency ranges are chosen conditionally and related to the resonance frequencies of the HLCF.

At low frequencies, the inductance of the main foil L_m provides the lowest impedance. Current in the main foil is zero because $R_{out} = \infty$. Current in the auxiliary foil is negligible because the capacitance C_b provides large impedance. Therefore, a low frequency voltage applied at the input terminal appears without changes at the output terminal. Along with the frequency increasing, capacitive coupling via C_b becomes dominating. It happens at frequency

$$f_{res1}=\frac{1}{2\pi\sqrt{L_aC_b}}=\frac{1}{2\pi\sqrt{LC_b}}, \tag{4}$$

after which the attenuation increases with the slope -40 dB/dec.

It is interesting to mention that, according to the transfer function, a low frequency resonance takes place between the capacitance C_b and the auxiliary foil inductance L_a, but not the main foil inductance L_m. Anyway, the equivalent circuit presented in Fig. 6(a) seems to be reasonable for the design.

At intermediate frequencies (Fig. 6(b)), the capacitance C_b becomes dominant and the current flows through the auxiliary foil. The inductance of the auxiliary foil prevents damping,

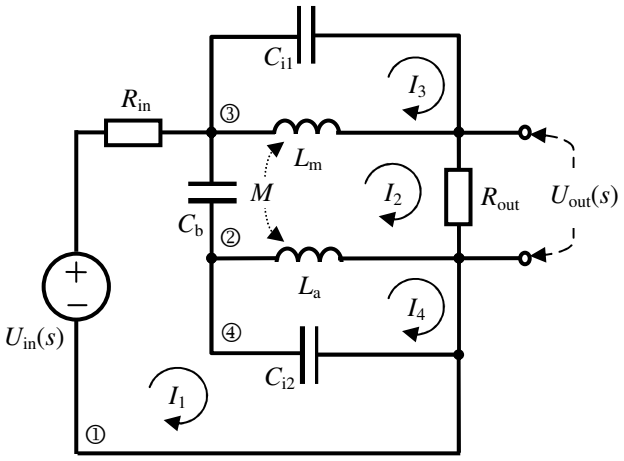

Fig 4. Equivalent circuit for the matrix of the impedances

since its impedance at intermediate frequencies is quite large. However, in accordance with the Lenz law, the current in the auxiliary foil creates a current of the opposite direction in the main foil. This is the same as mutual inductance placed into the main foil with the polarity reversed relatively the applied voltage $U_{in}(s)$. This coupling through the mutual inductance becomes dominant at frequency

$$f_{res2}=\frac{1}{2\pi\sqrt{(L_a-M)C_b}}=\frac{1}{2\pi\sqrt{(L-M)C_b}}. \tag{5}$$

After the frequency f_{res2} attenuation slope becomes about 0 dB/dec. The level of the attenuation at the intermediate frequencies increases with the mutual coupling between foils. Implementing equation (5) to Fig. 5, we can see that the higher the mutual inductance between foils is, the better the attenuation at intermediate frequencies will be.

$$W_{out}(s)=\frac{U_{out}(s)}{U_{in}(s)}=\frac{a_4s^4+a_3s^3+a_2s^2+a_1s^1+a_0s^0}{b_5s^5+b_4s^4+b_3s^3+b_2s^2+b_1s^1+b_0s^0}, \tag{3}$$

where
$$a_4=(M^2-L_mL_a)\cdot(C_b+C_{i2})\cdot C_{i1}R_{out},$$
$$a_3=0,$$
$$a_2=\left[MC_b-L_mC_{i1}-L_a(C_b+C_{i2})\right]R_{out},$$
$$a_1=0,$$
$$a_0=-R_{out},$$

$$b_5=(M^2-L_mL_a)\cdot C_bC_{i1}C_{i2}R_{in}R_{out},$$
$$b_4=(M^2-L_mL_a)\cdot\left\{\left[(C_{i1}+C_b)C_{i2}+C_bC_{i1}\right]R_{in}+\left[(C_{i2}+C_b)C_{i1}R_{out}\right]\right\},$$
$$b_3=(M^2-L_mL_a)\cdot(C_{i2}+C_b)-(L_mC_{i1}+L_aC_{i2})C_bR_{in}R_{out},$$
$$b_2=2MC_bR_{in}-L_m\cdot\left[(C_{i1}+C_b)\cdot R_{in}+C_{i1}R_{out}\right]-L_a\cdot(C_{i2}+C_b)\cdot(R_{in}+R_{out}),$$
$$b_2=-(L_m+C_bR_{in}R_{out}),$$
$$b_2=-R_{out}.$$

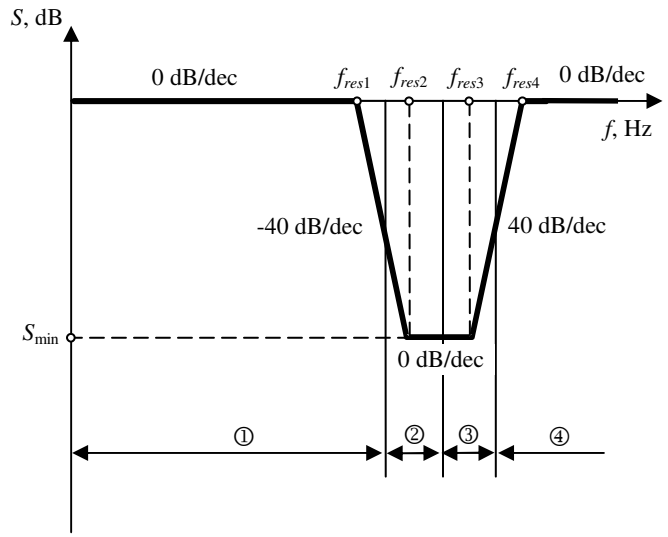

Fig 5. Asymptotic Bode plot of the HLCF (one phase). Range 1: low frequencies. Range 2: intermediate frequencies. Range 3: high frequencies. Range 4: frequencies over the working range of the HLCF.

From low to intermediate frequencies components C_{i1}, C_{i2} in equation (3) can be replaced with zero. Then, the transfer function becomes

$$W_{out}(s) = \frac{(L-M)C_b s^2 + 1}{LC_b s^2 + 1} \tag{6}$$

At high frequencies the impedance provided by the capacitance C_b is negligible (Fig. 6(c)). However, the intra capacitance of the main foil C_{i1} worsens the attenuation. The effect of the intra capacitance of the auxiliary foil C_{i2} is also negligible. Starting at frequency

$$f_{res3} = \frac{1}{2\pi\sqrt{(L+M)C_{i1}}} \tag{7}$$

the attenuation falls down with the slope 40 dB/dec.

Finally, at frequency f_{res4} a new resonance takes place and the attenuation becomes 0 dB/dec. In order to find this frequency, the denominator of equation (3) should be equated to zero, assuming capacitance C_b infinite. Then, the following equality can be obtained:

$$\left(L^2 - M^2\right)\cdot C_{i1}\cdot s^4 + L\cdot s^2 + 1 = 0 \tag{8}$$

.

Equation (8) gives

$$f_{res4} = \frac{1}{2\pi}\cdot\sqrt{\frac{L + \sqrt{L^2 - 4\cdot\left(L^2 - M^2\right)\cdot C_{i1}}}{2\cdot\left(L^2 - M^2\right)\cdot C_{i1}}} \tag{9}$$

.

If to take into account that $L^2 >> 4\cdot\left(L^2 - M^2\right)\cdot C_{i1}$ equation (9) becomes

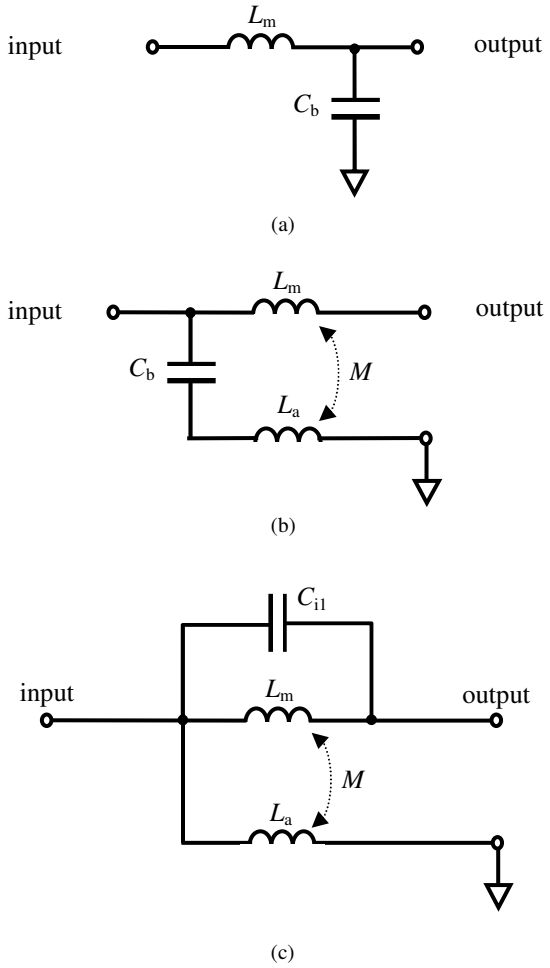

Fig 6. Equivalent circuits of the HLCF across the frequency domain. (a) at low frequencies. (b) at intermediate frequencies. (c) at high frequencies.

$$f_{res4} \approx \frac{1}{2\pi}\cdot\sqrt{\frac{L}{\left(L^2 - M^2\right)\cdot C_{i1}}} \tag{10}$$

.

Equation (10) indicates that the higher is the mutual inductance, the wider is the frequency range of attenuation.

After frequency f_{res4} the HLCF can be roughly described as an intra capacitance of the main foil C_{i1}.

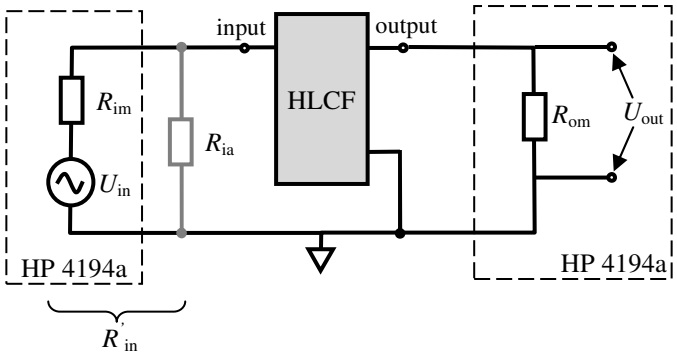

Fig 7. Obtaining the Bode plots with an HP 4194a frequency analyzer.

V. Measured, Simulated and Calculated Results

Inductance, capacitance, resistance and Bode plot measurements were performed with HP 4194a impedance and gain-phase analyzer, which allows impedance measurement in the frequency range from 100 Hz to 40 MHz and gain-phase measurement in the range from 10 Hz to 100 MHz. For gain-phase measurements the analyzer comprises two precision resistances: the input resistance is non-selectable R_{im} = 50 Ω, whereas the output resistances can be selected whether R_{om} = 50 Ω or R_{om} = 1 MΩ. In real drive, output impedance is usually more than 1 kΩ, whereas input impedance is relatively small. Therefore, in order to prevent damping of the resonances in measured frequency responses, additional resistance R_{ia} was added in the test setup as shown in Fig. 7 and the output resistance of the analyzer was chosen equal to R_{om} = 1 MΩ. The value of additional resistor R_{ia} = 1 Ω was selected to provide small input resistance $R'_{in} = \frac{R_{im} \cdot R_{ia}}{R_{im} + R_{ia}} = \frac{50 \cdot 1}{50 + 1} \approx 1\ \Omega$ (calculated in accordance with Thévenin's theorem). It was also measured beforehand that resistance R_{ia} keeps stable values over the frequency range 10 Hz – 30 MHz.

One phase unit of the investigated hybrid LC filter prototype is shown in Fig. 8. It was designed in accordance with recommendations given in [1] and [2]: small height and large diameter lead to low cost and price. Large diameter, however, complicates the installation of the filter phase units. Filter one phase unit dimensions (excluding terminals) for 75 A, 400 V drive are: height h = 80 mm, outside diameter D_{out} = 410 mm. In a real application, phase units of such a hybrid LC filter can be placed, for example, on top of each other even though the filter then becomes somewhat non-symmetrical. The filter is made of aluminium foils (the thickness of the main foil is 0.5 mm, the thickness of the auxiliary foil is 0.1 mm), separated by 0.5 mm Nomex insulator. Measured electrical parameters at 100 Hz: main foil inductance L_m = 126 μH, auxiliary foil inductance L_a = 126 μH, mutual inductance M = 124 μH, capacitance between foils C_b = 158 nF, intra capacitance of the main foil (auxiliary foil is not earthed) C_{i1} = 0.15 nF, intra capacitance of the auxiliary foil C_{i2} = 0.15 nF. In accordance with recommendation in [1], the intra capacitance of the main foil for simulation is 1/15 of its measured value or C_{i1} = 0.01 nF.

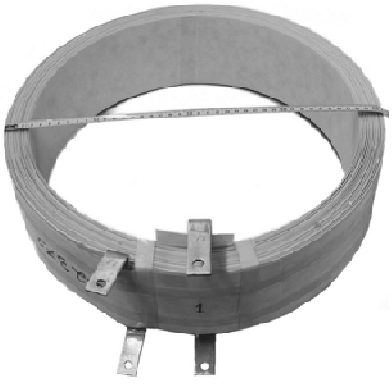

Fig 8. Investigated hybrid LC filter 75 A, 400 V prototype with 410 mm diameter.

A comparison of measured, simulated and calculated results is given in Fig. 9. These results show that the measured and simulated frequency responses are quite similar, especially in frequency range up to 2 MHz. Measured resonances are damped better than simulated ones. This is because only the DC resistances, not AC resistances, of the foils were taken into account in the simulations. Distributed nature of the hybrid LC filter is also not taken into account in the lumped model used for frequency analysis. These facts explain the differences between measured and simulated responses at intermediate and high frequencies (the lengths of the foils of the prototype are about 17 m, i.e. a transmission line effect can be expected). On the other hand, the lumped model simplifies significantly the frequency behavior of the HLCF analysis given in section IV. Differences at frequencies higher than 2 MHz can also be explained by the inserted impedances of the connection wires which weren't taken into account in simulations.

The asymptotic frequency response in Fig. 9 is built using equations (4), (5), (7) and (10). The simulated and calculated curves presented in Fig. 9 are, in fact, derived from the same equation. The differences between simulated and calculated plots are explained by the fact that asymptotic response does not take into account signal amplification (or attenuation) at resonance frequencies.

It is evident that the asymptotic frequency response describes the HLCF model behaviour quite well. Such a simple approach can be used, for example, in MS Excel or other similar programs for quick HLCF properties estimation.

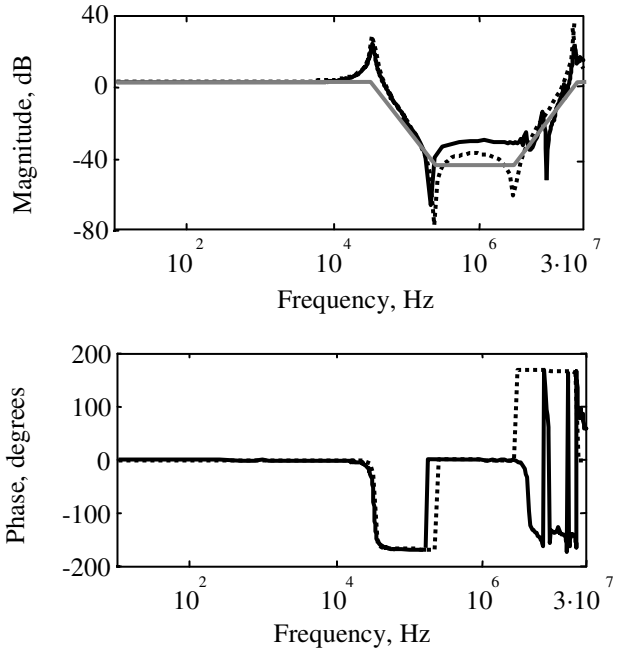

Fig 9. Frequency response comparison: ▬ – measured, ▪▪▪ – simulated, ▬ – calculated.

VI. Conclusion

This paper considers the new type of electrical filter, called hybrid LC filter, which can be used in power electronic drives replacing traditional d*u*/d*t* filters. Such a filter reminds a conventional foil choke, but an additional auxiliary winding is integrated between main winding turns. This winding can be connected to a neutral potential of the drive. The construction proposed allows transforming the internal stray capacitance of the conventional foil choke into a useful capacitance which contributes to the DM and CM noises' attenuation.

However, auxiliary foil integration complicates the hybrid LC filter analysis, since it creates essential mutual inductance which influences the filter frequency responses. In combination with modern scientific software, nowadays methods of the electric circuits' analysis provide extensive possibilities for the investigation of the devices with mutual coupling.

Thus, hybrid LC filter has a complex representation in the frequency domain. At low frequencies the hybrid LC filter can be considered as a simple LC filter. At intermediate and high frequencies the mutual inductance between the main and auxiliary foils plays a very important role: the higher the mutual inductance is, the better is the attenuation. Therefore, theoretically, the main and auxiliary windings of the hybrid LC filter should be placed as close to each other as possible. This is also desirable in order to increase the useful capacitance between foils. However, in practice the decreasing of the distance between the windings is limited by the voltage stress applied to the insulation layer. Anyway, in order to provide the best possible performance, winding and insulation layers should be coiled as tight to each other as possible.

Equations proposed in the paper are convenient for the hybrid LC filter properties estimation with the asymptotic Bode plots. With that, the transfer function of the hybrid LC filter proposed in the paper can be used for the hybrid LC filter analysis in time and frequency domains.

References

[1] V. Dzhankhotov, "Hybrid LC filter for power electronic drives: theory and implementation," D.Sc. dissertation, Dept. Elect. Eng., Lappeenranta, Finland, 2009.

[2] V. Dzhankhotov, J. Pyrhönen, P. Silventoinen, M. Kuisma and T. Minav, "A New Passive Hybrid Air-Core Foil Filter for Modern Power Drives," *IEEE Trans. Ind. Electron.,* to be published.

[3] A. von Jouanne and P. Enjeti, "Design considerations for an inverter output filter to mitigate the effects of long motor leads in ASD applications," *IEEE Trans. Ind. Appl.*, vol. 33, no. 5, pp. 1138-1145, Sep./Oct. 1997.

[4] P. Finlayson, "Output filters for PWM drives with induction motors," *IEEE Industry Application Magazine*, vol. 4, no. 1, pp. 46–52, Jan./Feb. 1998.

[5] S. Lee and K. Nam, "An overvoltage suppression scheme for AC motor drives using a half DC-link voltage level at each PWM transition," *IEEE Trans. Ind. Electron.,* vol. 49, no. 3, pp. 549–557, Jun. 2002.

[6] S. Lee and K. Nam, "Overvoltage suppression filter design Methods based on voltage reflection theory," *IEEE Trans. Pow. Electron.*, vol. 19, no. 2, pp. 264-271, March 2004.

[7] K. Ben Smida, P. Bidan, T. Lebey, F. Ben Ammar and M. Elleuch, "Identification and time-domain simulation of the association inverter–cable–asynchronous machine using diffusive representation", *IEEE Trans. Ind. Electron.,* vol. 56, no. 1, pp. 250–258, Jan. 2009.

[8] H. Paula, D. de Andrade, M. Chaves, J. Domingos and M. de Freitas, "Methodology for Cable Modeling and Simulation for High-Frequency Phenomena Studies in PWM Motor Drives," *IEEE Trans. Pow. Electron.,* vol. 56, no. 1, pp. 250–258, Jan. 2009.

[9] D. Rendusara and P. Enjeti, "An improved inverter output filter configuration reduces common and differential modes dv/dt at the motor terminals in PWM drive systems," *IEEE Trans. on Pow. Electron.*, vol. 13, no. 6, pp. 1135-1143, Nov. 1998.

[10] D. Busse, J. Erdman, R. Kerkman, D. Schlegel and G. Skibinski, "Bearing Currents and Their Relationship to PWM Drives," *IEEE Trans. Pow. Electron.*, vol. 12, no. 2, pp. 243-252, March 1997.

[11] A. Muetze and A. Binder, "Calculation of circulating bearing currents in machines of inverter-based drive systems," *IEEE Trans. Ind. Electron.,* vol. 54, no. 2, pp. 932–938, Apr. 2007.

[12] A. Muetze and A. Binder, "Practical rules for assessment of inverter-induced bearing currents in inverter-fed AC motors up to 500 kW", *IEEE Trans. Ind. Electron,* vol. 54, no. 3, pp. 1614–1622, Jun. 2007.

[13] A. Muetze and A. Binder, "Techniques for Measurement of Parameters Related to Inverter-Induced Bearing Currents," *IEEE Trans. Ind. Appl.*, vol. 43, no. 5, pp. 1274–1283, Sep/Oct. 2007.

[14] A. Binder and A. Muetze, "Scaling Effects of Inverter-Induced Bearing Currents in AC Machines", *IEEE Trans. Ind. Appl.*, vol. 44, no. 3, pp. 769–776, May/Jun. 2008.

[15] B. Mirafzal, G. Skibinski, R. Tallam, D. Schlegel and R. Lukaszewski, "Universal Induction Motor Model With Low-to-High Frequency-Response Characteristics," *IEEE Trans. Ind. Appl.*, vol. 43, no. 5, pp. 1233–1246, Sep./Oct. 2007.

[16] L. Palma, M. Todorovic, P. Enjeti, "Analisys of common-mode voltage in utility-interactive fuel cell power conditioners," *IEEE Trans. Ind. Electron*., vol. 56, no. 1, pp. 20–27, Jan. 2009.

[17] X. Chen, D. Xu, F. Liu and J. Zhang, "A novel inverter-output passive filter for reducing both differential- and common-mode dv/dt at the motor terminals in PWM drive systems," *IEEE Trans. Ind. Electron.*, vol. 54, no. 1, pp. 419–426, Feb. 2007.

[18] M. Kuisma, V. Dzhankhotov, J. Pyrhönen and P. Silventoinen, "Air-cored common mode filter with integrated capacitors", in *Proc. of European Conference on Power Electronics and Applications*, Barcelona, 2009.

[19] J. Pyrhönen, P. Silventoinen, M. Kuisma and V. Dzhankhotov. "A filter appliance for a multiphase electrical converter device", E.U. patent application 2 251 964, November 17, 2010.

[20] S. Wang and F. Lee, "Analysis and applications of Parasitic Capacitance Cancellation Techniques for EMI suppression," *IEEE Trans. Ind. Electron,* vol. 57, no. 9, pp. 3109–3117, Sep. 2010.

[21] V. Khudyakov, V. Khabuzov and A. Vasiliev, "Transfer function and frequency responses obtaining of the voltage converter noise filter" (in Russian), *Power Electronics,* vol. 2, pp. 96–99, 2006.

Valentin Dzhankhotov, born in Saint-Petersburg, Russian Federation, in 1977. He received Ph.D. degree (control systems) in 2004 from Saint-Petersburg State Electrotechnical University (LETI). In 2009 he received D.Sc degree (electrical engineering) from Lappeenranta University of Technology (LUT), Finland. From 2000 he is the lecturer at Control Systems Department at LETI. From 2008 he is R&D Researcher at The Switch Drive Systems Oy, Lappeenranta, Finland. From 2010 he is Researcher of the Department of Electrical Engineering at LUT. Current research interests are in the field of high power drives, especially electrical filters and control.

Juha Pyrhönen, born in 1957 in Kuusankoski, Finland, received the Doctor of Science (D.Sc.) degree from Lappeenranta University of Technology (LUT), Finland in 1991. He became an Associate Professor of Electrical Engineering at LUT in 1993 and a Professor of Electrical Machines and Drives in 1997. He is currently the Head of the Department of Electrical Engineering, where he is engaged in research and development of special electric motors and drives. His current interests include different permanent magnet synchronous machines, induction

motors and solid-rotor high-speed induction machines and drives.

Pertti Silventoinen was born in 1965 in Simpele, Finland. He received the Doctor of Science (D.Sc) degree from Lappeenranta University of Tecnology (LUT), Finland in 2001.

He became a Professor of Applied Electronics in 2004. He is currently the Head of Degree Program in Electrical Engineering in the Institute of LUT Energy. His current interests include power electronic systems in various applications.

Mikko Kuisma was born in Finland in 1971. He received his M.Sc. degree in electrical engineering and control systems in 1997 and D.Sc. degree in electronics in 2004 from Lappeenranta University of Technology, Finland. Since 1995, he has been working as a research engineer and lecturer at Lappeenranta University of Technology. His research interests include EMC, power electronics, analog signal processing, and engineering education. Recent research topics include EMC in power electronics, signal processing in biosensors, and academic curriculum in higher education. Dr. Kuisma is currently an associate professor of applied electronics at Lappeenranta.